Article

Heavy Rainfall Events in Selected Geographic Regions of Mexico, Associated with Hail Cannons

Victor M. Rodríguez-Moreno [1,*] and Juan Estrada-Ávalos [2]

1 INIFAP, National Institute for Forestry, Agriculture and Livestock Research, Experimental Field Station Pabellon, Km 32.5 Highway Aguascalientes-Zacatecas, Pabellon de Arteaga ZP 20670, Mexico
2 INIFAP, National Institute for Forestry, Agriculture and Livestock Research, CENID RASPA, Km 6.5 Left Margin of Sacramento Cannel, Gomez Palacio ZP 35140, Mexico; estrada.juan@inifap.gob.mx
* Correspondence: rodriguez.victor@inifap.gob.mx; Tel.: +52-018000882222

Abstract: In this article, we document the use of hail cannons in Mexico to dispel or suppress heavy rain episodes, a common practice among farmers, without scientific evidence to support its effectiveness. This study uses two rain databases: one compiled from the Global Precipitation Measurement (GPM) mission and the other generated with the implementation of the Weather Research and Forecasting (WRF) model. The aim is to explore the association between heavy rain episodes and hail cannon locations. The analysis includes two geographic features: a pair of coordinates and a 3 km radius area of influence around each hail cannon. This dimension is based on the size and distribution of the heavy rainfall events. This study analyzes four years of half-hourly rain data using the Python ecosystem environment with machine learning libraries. The results show no relationship between the operation of hail cannons and the dissipation or attenuation of heavy rainfall events. However, this study highlights that the significant differences between the GPM and WRF databases in registering heavy rain events may be attributable to their own uncertainty. Despite the unavailability of ground-based observations, the inefficiency of hail cannons in affecting the occurrence of heavy rain events is evident. Overall, this study provides scientific evidence that hail cannons are inefficient in preventing the occurrence of heavy rain episodes.

Keywords: WRF; remote sensing; hail cannon; heavy rainfall

1. Introduction

The history of building devices for weather modification is long. In 1880, an Italian professor of mineralogy stated that it was conceivable that the formation of hailstones could be prevented by injecting smoke particles (to serve as condensation nuclei) by means of cannons fired at thunderstorms [1]. The concept of using cannons to provide nuclei to suppress hail was experimented with in 1896 by M. Albert Stiger, the Burgomaster of Windisch-Feistritz (a municipality in the province of Syria, Austria) and a famous wine grower [2]. Stiger was inspired by a desire to help relieve the enormous hail losses in his province [1]. Using backyard tests over a period of several years, he had evolved a vertical-pointing muzzle-loading mortar, resembling a very large upright megaphone. When fired, it produced a large smoke ring that whistled loudly as it rose to a height of typically 300 m above the cannon [1]. This reference may be one of the first that documented the cloud seeding nuclei through a seeding device. Meanwhile, numerous concepts and hypotheses as to how seeding works were purported [3]. By using the analogy of a megaphone to describe a hail cannon can be a helpful way to convey the basic concept, but it is important to note that hail cannons are more complex devices, designed for a specific purpose. The analogy might be useful to provide a simple understanding, especially for a general audience, but it does not capture all the nuances of how hail cannons work. As if a megaphone amplifies sound to make it louder, allowing it to travel farther, a hail cannon uses a loud noise, often a shockwave, to disrupt the formation of hailstones. The shockwaves created by the hail

cannon act as a disturbance in the atmosphere, interfering with the process that leads to the formation of hail. Just as a megaphone's sound is directed in a specific direction, hail cannons are usually aimed at the area where crops need protection. The goal is to disrupt hail formation in that specific, localized region. The tight relationship between crop production systems and rainfall events is obvious, in essence, in areas where agricultural activities are dependent on rain-fed systems. Rainfall events are particularly important in agricultural production systems: extreme precipitation causes numerous issues, including flooding, crop damage, health hazards, water contamination [4–6], and sediment transport.

Extreme rainfall events negatively impact the primary economic sector. The last decade has witnessed an increase in the number of extreme weather events globally [7]. In addition, the economic output around the world is at an all-time high in terms of production and profitability. However, global warming and extreme weather are modifying the natural ecosystem and the human social system, leading to the appearance of extreme climate events that have an adverse impact on the world economy (ibidem). In particular, in production systems, extreme weather events can reduce crop yields, leading to reduced productivity across various industries [8] (i.e., by breaking branches, stems and leaves; and causing early or damaged fruits). Moreover, extreme weather events can lower vegetation net primary productivity rates, diminish water harvest, and result in associated soil effects (i.e., increased erosion rates; affecting pedogenic processes; and washing away soil organic carbon, soil nutrients, and organic matter). In addition, these events can promote the appearance of soil–plant pathogens, i.e., fungus, phytoplasma, and nematodes. Therefore, the economic impacts can be significant, with some estimates suggesting that the costs of extreme weather events are expected to increase in the coming years.

The atmospheric conditions accompanying extreme precipitation events have been well-documented, and no single factor has been found to correlate perfectly with heavy rainfall [9]. According to [10], extreme weather conditions such as heat waves, droughts, and floods have been shown to have a significant impact on production economics. These events can disrupt supply chains. Heavy rain events, severe convective storms, and overall changes in spatial distribution events and their intensity are now regularly observed. Sadly, these disasters disproportionately harm poor people in low-income regions that have had minimal contributions to the buildup of greenhouse gasses. The summer of records has been characterized by extreme heatwaves sweeping across the globe, as well as by other natural disasters, such as flooding, hurricanes, and wildfires [11]. These events can occur anywhere, but are almost exclusively observed during the summer season, and are usually accompanied by heavy rain, strong winds, lightning, and hail [12]. It is important to note that the timing and intensity of severe weather events can be influenced by regional climate patterns, local geography, and atmospheric conditions. While summer is a common season for severe weather in many places, it is not a universal rule. The association between severe weather and the summer season can vary depending on the geographic location and the increased warmth and humidity during these months, creating conditions favorable for the development of convective storms; hurricanes and tropical storms can bring heavy rainfall, strong winds, and storm surges, particularly during the late summer and early fall. The summer months can also see an increase in heavy rainfall events, which is often associated with slow-moving or stalled weather systems that can dump large amounts of rain over a specific area.

In Mexico, heavy rainfall events during the summer season are not uncommon, and they are often associated with the North American Monsoon (NAM). The NAM typically occurs from June to September and brings a significant increase in moisture to the region, leading to convective storms and heavy rainfall.

- The monsoon typically begins in southern Mexico in early June and progresses northward to the southwestern United States by early July [13,14]. This seasonal shift in wind patterns brings moist air from the Gulf of Mexico and the Gulf of California into the region. As this moist air rises, it cools and condenses, leading to the development of convective storms.

- The intensity and frequency of heavy rainfall events can vary across different regions of Mexico. Coastal areas, mountainous terrain, and inland plains may experience different patterns of rainfall.
- The combination of intense rainfall and the topography of some regions can increase the risk of flash floods and river flooding.
- Mexico is also prone to tropical cyclones (hurricanes and tropical storms), especially on the Pacific and Atlantic coasts. These systems can bring heavy rainfall, strong winds, and storm surges.

Hail cannons are commonly used in agricultural regions to protect crops from hailstorms [15]. In Mexico, their installation and operation are widely accepted measures among agricultural producers, who believe that these devices can protect against extreme weather events by cracking hailstones through the generation of shockwaves. The speed at which a shockwave propagates can vary, depending on several factors, including the medium through which it travels. In the atmosphere, the speed of sound, and therefore the speed of a shockwave, is influenced by factors such as temperature and pressure. In general, the speed of sound in the Earth's atmosphere at sea level is approximately 343 m per second under standard conditions (at 20 degrees Celsius). However, this speed can change with variations in temperature and pressure. However, there is no scientific evidence to support this unproven technological solution. While it is widely believed that once the hailstone is broken up into small pieces, it will melt and reach the ground as raindrops, the scientific community has not yet demonstrated if hail cannon sound waves cause these cracking effects.

The effectiveness of hail cannons is still unclear, and the scientific opinion on their use as a weather modification tool is debatable. For example, Bordeaux wine producers had an elaborate system in place to protect their vines from hail: a network of cannons that generated shockwaves to limit the formation of large hailstones. Nevertheless, the proprietors of the châteaux expressed dissatisfaction, as the system proved ineffective in safeguarding their crops amid recent storms in the region [16].

The aim of this research is to investigate the spatial relationship between heavy rainfall episodes and hail cannon device locations by applying spatial analysis techniques. Specifically, we aim to analyze the geographic distribution and clustering of heavy rainfall events relative to the spatial distribution of hail cannon installations. Through this analysis, we seek to elucidate any potential spatial patterns or correlations that may exist between the presence of hail cannons and the occurrence of heavy rainfall, thereby contributing to a better understanding of the localized meteorological effects of hail cannon usage. To the best of our knowledge, previous studies have not specifically addressed this relationship by using grid data arrays to determine whether any reduction, dissipation, or suppression of heavy rainfall events associated with the location of hail cannons have occurred.

This study does not focus on cloud physics but instead uses satellite images and modeled data of rain to identify the potential relationship between the hail cannon location and convective clouds on a wide scale.

2. Materials and Methods

2.1. Study Area

This study covers three relevant agricultural regions in Mexico, where 51 monitoring sites are located, and the data coordinates were shared with many reserves from the device owners. The state of Michoacán (MICH) has 22 locations, the state of Jalisco (JAL) has 14 installed devices, and the state of San Luis Potosí (SLP) has 15 hail cannons (Figure 1, shown inside Figure 1B). The cannons' areas of influence include large-scale farms and small anthropogenic constructions that are affected by heavy rain events. Due to the reluctance of the owners to share the schedule of operations, we assume that the devices operate at short intervals (4 to 7 s) for the entire period since the storm approaches the cannon's location until it has passed the protected area. The surface protected by such an

isolated system is a circle with a radius of approximately 500 m, and the effectiveness of the protection decreases as the distance from the installation location increases [17].
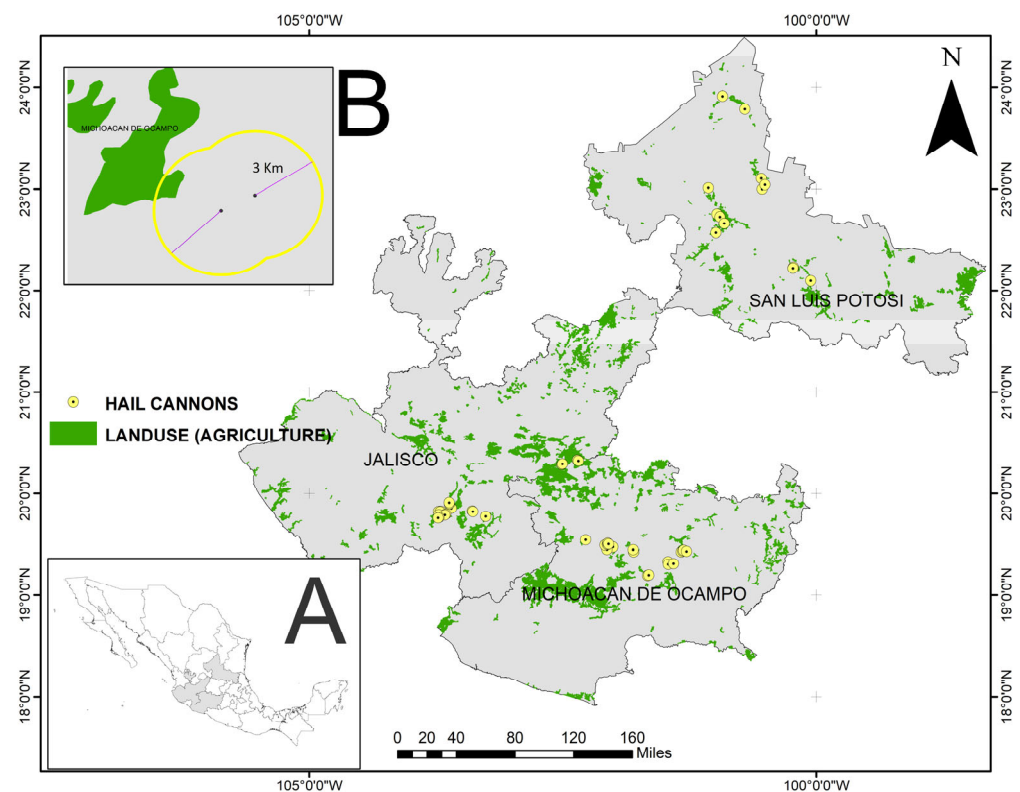

Figure 1. Geospatial distribution of hail cannons and schematization of point coordinates and their area of influence (**B**). Subfigure (**A**) is a representation of the study region in Mexico.

Figure 1 shows the geospatial distribution of hail cannons in three agricultural regions in Mexico. The figure also includes a schematic representation of the point coordinates and the proposed area of influence, which is a 3 km buffer around each hail cannon. This distance is arbitrary and has no previous scientific basis, as manufacturers typically advertise a protection area of 500 m around the device. However, the 3 km buffer was chosen to cover at least a 5×5 pixels matrix, with the centroid pixel matching the position of the cannon. This buffer is considered the area where heavy rain events could potentially be affected by the operation of the hail cannon. The meteors in the Jalisco and Michoacán zones are born at a latitude of $15°$ N, approximately. Generally, the first meteors travel towards the west, moving away from national coasts, while those formed from July onwards, which are of greater power, usually follow a parabolic path. The shape of the Mexican Pacific coast makes them travel parallel to the coast and, when taking the second branch of the trajectory, they penetrate inland north of Cabo Corrientes, affecting the states of Nayarit, Sinaloa, Sonora, and the extreme southern part of the Baja California Peninsula. However, during its first branch, it will bring torrential rains to the coasts of Chiapas, Oaxaca, Guerrero, Michoacán, Colima, and Jalisco, which are located in the hurricane's dangerous semicircle [18]. The San Luis Potosí region is affected by the events originating from the second matrix zone. This zone is located in the southwestern portion of the Gulf of Mexico, in the warm waters that form the so-called Campeche Sound. It becomes active in the first fortnight of June, at a latitude close to $20°$ N. The initial meteors, characterized as rainy systems, run parallel to the coast of Veracruz and gradually intensify in such a way that those born from July onwards reach full development (ibidem).

2.2. Dataset Description

The dataset used in this study covers a period of four years, from January 2014 to January 2018. It includes 140,256 records of rainfall data collected every 30 min. The data were declared external in x, y, and z form and were used to approximate the function f: z = f(x, y), which returns a function that uses spline interpolation to find the value of new points. The dataset was integrated from two databases, the WRF and GPM databases, which were both 10 km in spatial resolution and were composed of independent and identically distributed data. To frame the dataset on geographic features, scripts were written in the Pandas library, a data analysis and manipulation tool built on top of the Python programming language [19]. The importance of Python, particularly through the Pandas library, lies in its ability to handle datasets and the capabilities required by programming experts. Emphasizing the ability to write and execute custom algorithms adds a layer of skill and control, showcasing a deeper understanding of data analysis and manipulation. Custom algorithms can be tailored to specific research needs, providing a more flexible and nuanced approach compared to off-the-shelf models. This demonstrates a higher level of expertise and adaptability in dealing with the unique challenges or requirements of a given dataset or research question. Statistical downscaling by multiple regressions to a 1 km thematic grid surface was applied on both databases. The 3 km area of influence buffer was used as a vector mask to obtain the zonal statistics, excluding the central pixel from the statistical zone analysis (Figure 2).
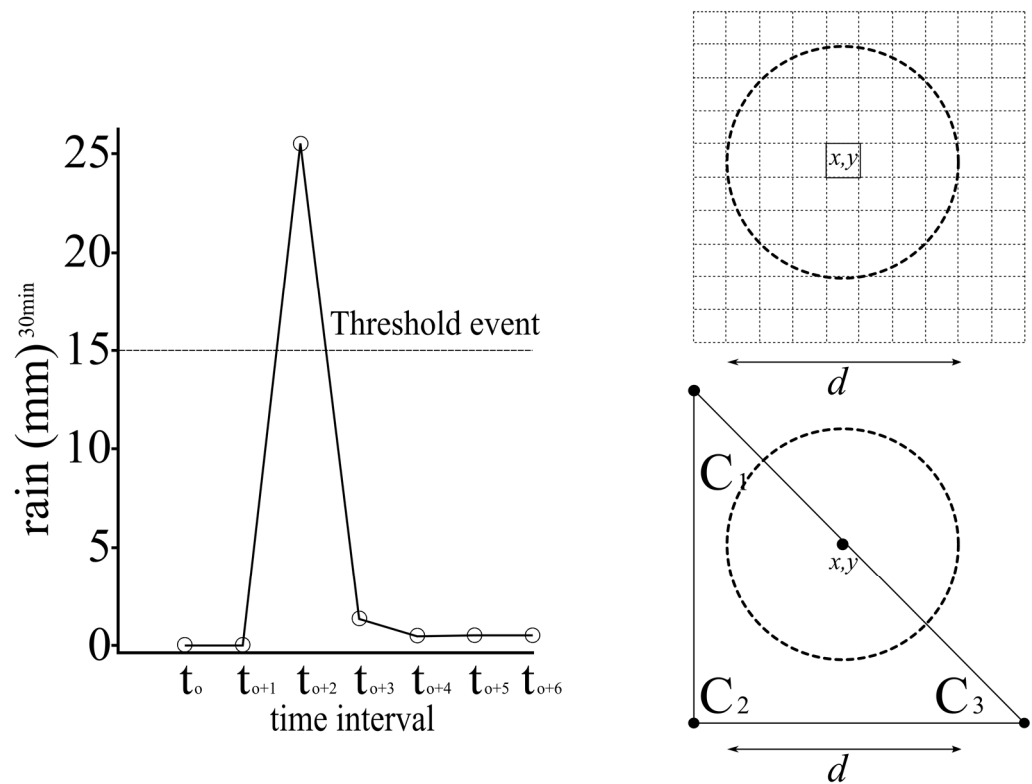
Figure 2. Schematization of a heavy rainfall event; the 3 km radius of area of influence was represented as a regular surface of a 1 km grid (**upper right**) in a matrix of 5 × 5 pixels, while the point coordinates represent the hail cannon's location. The algorithm reads data at time interval t_0, then the six subsequent intervals (t_0 to t_6); the reading procedure restarts with each new datapoint (**left**). The nearest centroid to the geographic point x, y, z data is represented by the (**down right**) triangle vertex (C_1, C_2, and C_3), while the line segment "d" and the dotted line circumference represent the 3 km area of influence.

2.3. Description of a Heavy Rainfall Event

In rainfall data analysis, the statistical context of improving data quality and reliability starts by filtering out values of 0 mm and those less than 0.1 mm. This is because rainfall measurements are typically recorded in discrete units (e.g., millimeters), and values of 0 mm or very small values may represent non-measurable or negligible precipitation events. Removing such values can help ensure that the analysis focuses on significant rainfall events. Excluding non-plausible data points, such as extreme outliers or erroneous measurements, is essential for improving the quality of the dataset. Non-plausible data points could arise from measurement errors, instrument malfunctions, or other factors. By filtering out these data points, we can reduce the likelihood of biased results and ensure that the analysis is based on reliable data. This is especially important when dealing with large datasets, as it can help to reduce computational time and resources. The definition of a heavy rainfall event as at least 15 mm of precipitated water over 30 min is also a reasonable threshold, as it is in line with the definition provided by the IPCC (Intergovernmental Panel on Climate Change) Special Report on Extremes: "an extreme (weather or climate) event is generally defined as the occurrence of a value of weather or climate variable above (or below) a threshold value near the upper (or lower) ends (tails) of the range of observed values of the variable" [20]. According the National Weather Service of Mexico, a heavy rainfall event "is a heavy, abundant, sudden rain of short duration. It is characterized by the fact that the composition of droplets or solid particles is greater than the elements corresponding to other types of precipitation" [21]. It is important to establish a clear and consistent definition of what constitutes a heavy rainfall event in order to accurately analyze and compare data across different regions and time periods (Figure 2).

As schematized in Figure 2, the output of the algorithm is a binary thematic image that stores both 0's and 1's, indicating whether an extreme rainfall event has occurred or not. The 1 km grid surface is a downscaled grid of the original 10 km grid of the GPM and WRF databases and was half-hourly interpolated. The pixel value that matches with the hail cannon location is extracted from this array. The nearest centroid to the geographic point x, y, z data in the satellite-origin and re-scaled-origin databases is represented by the downright triangle vertex (C_1, C_2, and C_3), while the segment "d" and the dotted line circumference represent the 3 km area of influence.

2.4. GPM Database Description

The GPM mission is a satellite-based mission that provides measurements of precipitation from space every 3 h [22], with an unprecedented resolution of 0.1° and 30 min [23]. The GPM_3IMERGHH product, which was used in this study, is the third-level precipitation product of GPM and covers an area of ±60° N/S [22,24]. This product provides essential 2D, 3D, and/or 4D data on precipitation ranging from rain microphysics and snow particles to global patterns of precipitation. The GPM IMERG product is a similar precipitation product that combines microwave, infrared, and gauge estimates [25]. The GPM images were chosen because of their extended capability to measure light rain and falling snow, which account for significant proportions of precipitation at mid- and high-latitudes [23]. The output file format of HDF5 has a spatial coverage of −180°, −60°, +180°, and +60°, and a spatial resolution of 0.1° (~10 km).

2.5. WRF Database Description and Model Configuration

The Weather Research and Forecasting model with the Unified Environmental Modeling System (WRF-UEMS) version 3.2 [26] was used in this study to simulate half-hourly data at a spatial resolution output of 10 km. The WRF model configuration included 35 terrain-following vertical levels and several physics options, such as the BMJ (Betts-Miller-Janjić) cumulus scheme [27], the Thompson microphysics [28], the Mellor–Yamada–Janjić (MYJ) planetary boundary layer scheme [29], and the Noah land surface model (LSM; [30]). The BMJ scheme was chosen for its ability to improve rainfall prediction and show better features of cyclonic circulation [31]. However, it is relevant to emphasize that the BMJ

scheme is a cumulus parameterization scheme used in numerical weather prediction models, and its performance can vary under different atmospheric conditions and regions. It was designed to improve the representation of sub-grid scale convection, particularly in the tropics. While it has demonstrated success in capturing certain features of convective processes, its performance may not be consistent in all areas or for all weather scenarios. The effectiveness of a parameterization scheme such as BMJ can depend on factors such as the following:

- Geographic location. Different regions have distinct climatic and atmospheric characteristics. It is of general recommendation that schemes that perform well in one region may not perform as well in another, and local and regional re-parameterization is mandatory.
- Seasonal variation. The performance of parameterization schemes can be influenced by seasonal variations in atmospheric conditions.
- Model resolution. The resolution of the numerical model can also affect the performance of the parameterization schemes. Some schemes may be better suited for higher resolution models.
- Specific weather phenomena. The scheme may perform differently in capturing different types of weather phenomena (e.g., convective storms, tropical cyclones, temperature profile, etc.).
- Model configuration. The overall configuration of the numerical weather prediction model, including the choice of other parameterization schemes and model physics, can impact the results.

The Thompson microphysics scheme was chosen for its ability to generate cloud properties in proper conditions where hail events are possible. It is therefore more suitable to reproduce convective clouds, which more dominated by rain species typical of tropical clouds [32]. The Thompson microphysics scheme is a type of cloud microphysics parameterization used in atmospheric models, particularly in the context of cloud and precipitation processes. Like any parameterization scheme, its performance can be influenced by various factors, and its suitability may vary across different scenarios and geographic regions. As for the BMJ scheme, geographic and climatic variation can be sensitive; different regions may have distinct cloud and precipitation characteristics, and a microphysics scheme that performs well in one region may not be optimal for another. Another relevant factor to mention is the temperature and moisture regimes. Microphysics schemes are often designed to simulate processes such as cloud droplet activation, raindrop formation, and ice processes. Their performance can be influenced by the prevailing temperature and moisture conditions.

Recent review studies have shown that although many studies on the evaluation and comparison of PBL parameterization schemes have been undertaken, there is still no uniform conclusion on which PBL parameterization scheme performs best [33]. The MYJ planetary boundary layer (PBL) scheme is a widely used parameterization scheme in atmospheric models, particularly in numerical weather prediction and atmospheric research. It is designed to represent the processes occurring in the planetary boundary layer, which is the lowest part of the atmosphere influenced by the earth's surface. The MYJ scheme was selected because of its computational performance and its ability to perform well in complex terrain conditions such as Mexico [34]. The Noah Land Surface Model (LSM) is a widely used component in atmospheric models, and it plays a crucial role in representing interactions between the land surface and the atmosphere. The Noah LSM was chosen because of its ability to provide multi-options for atmospheric physical processes [35,36], its versatility for a range of applications across different spatial and temporal scales, and its balance between accuracy and computational efficiency. However, it has been reported to have biases in simulating runoff and snowmelt.

Pre-Processing the Dataset

Interpolation is a widely used technique in spatial data analysis, and it is used to estimate values for unsampled points. Deterministic methods, such as barycentric methods, space-partitioning methods, and splines, estimate the value at unknown points based on a weighted sum of the value at close points [37]. These methods do not use probabilistic theory [38] and create surfaces based on either the extent of similarity or the degree of smoothing [39]. On the other hand, stochastic methods, such as regression, local regression, and kriging, infer the value of the unknown point as the value at a point supposed to have similar features. The nearest neighbor interpolation assigns the value of the closest known observation to the unknown point [37]. In this study, two Python (v.3.6.2) scripts were written to perform a pre-processing task due to a) the considerable number of files and disk space, b) the allocation of hard disk drive resources to store temporary and final output files, and c) the need to map the necessary consumption of computing resources. The scripts were performed in two phases. First, the original files in native-NetCDF (Network Common Data Form) format were transformed to a plain text (CSV format; Comma Separated Values). Second, the GPM and WRF rainfall datasets that lay inside the spatial limits of this study were subset. The interpolated surfaces were created using the CSV files of the rainfall data and centroid coordinates.

In the output process, several libraries were used, including SciPy, NumPy, and GDAL/OGR, to pre-process and interpolate the rainfall data. The SciPy library [40] was used to fit a function to the rainfall data, and the NumPy library was used for N-dimensional array manipulation. The GDAL/OGR libraries were used for raster and vector data format translation and to access various vector file formats, including ESRI shapefiles, S-57, GeoJSON, SDTS, PostGIS, Oracle Spatial, and Mapinfo. To obtain statistics by area of influence, we used the zonal statistics function, which utilizes the NumPy and GDAL/OGR libraries. The zonal statistics function, following a raster-based method, is widely used in environmental and geophysical studies [41].
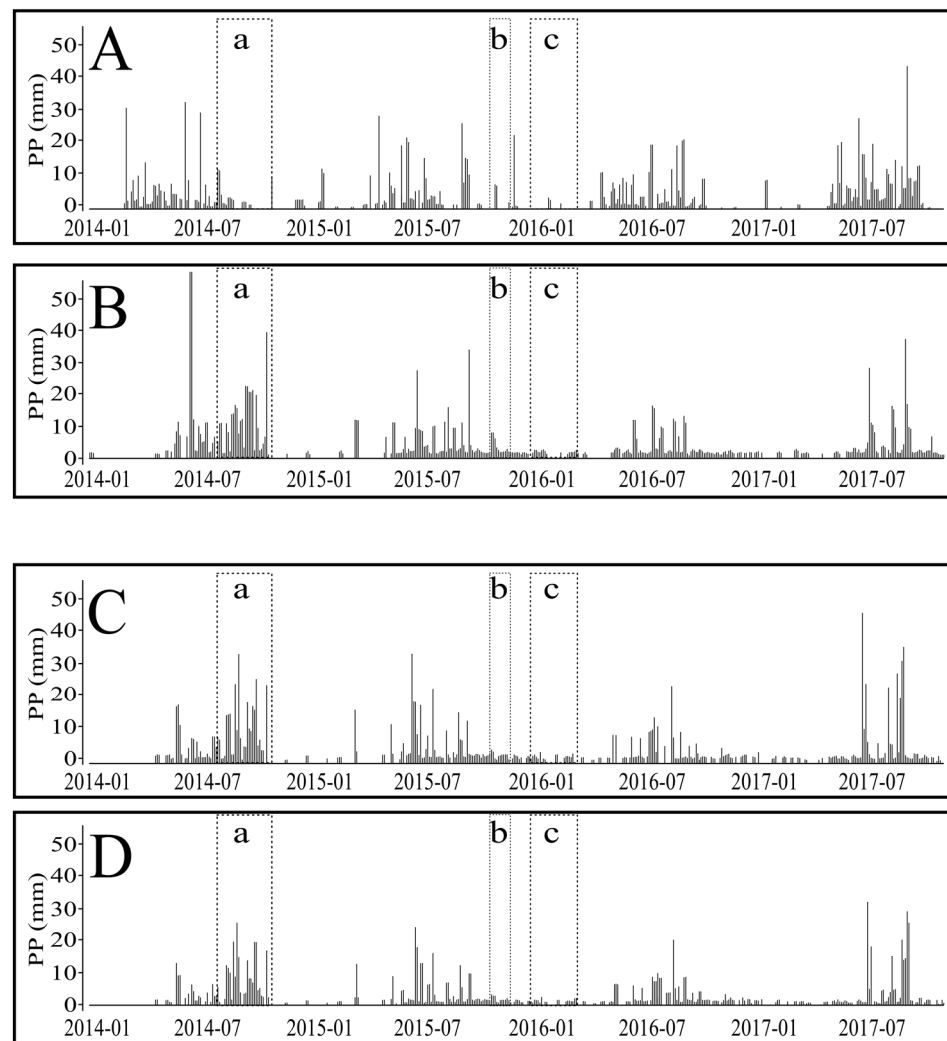
2.6. Rainfall Data

The four-year dataset was assembled at 30 min intervals; no missing data were observed (Figure 3). A few things to enhance are the following: cumulative rainfall data are presented daily because of the difficulty of representing in one figure the whole 30 min series data set. The number of anti-hail cannons was consistent throughout the period. As shown in Figure 4, the contrast between the GPM database and the WRF database, as well as the serial data period and the region, regarding the number and intensity of heavy rainfall events, was notable. Only cumulative rainfall above 15 mm is shown (Figure 4). Assigning a minimum volume of rain to categorize an event as heavy rainfall can depend on various factors, including regional climatology, local infrastructure, and the impact on the environment. In meteorology, heavy rainfall is often categorized based on the rate of precipitation, usually measured in millimeters per hour.

We suggested the 15 mm of rain in an interval of 30 min as a specific criterion that we can use, but the appropriateness of this threshold depends on the context. We are well aware that it is not uncommon for meteorological agencies to use thresholds like this, but they may also consider factors such as the local average rainfall, the drainage capacity of the area, and the potential for flooding.

In scientific terms, heavy rainfall is often defined in terms of intensity, such as rainfall rates exceeding a certain threshold over a specified time period. The specific thresholds can vary, and they may be established based on historical data, hydrological considerations, and the vulnerability of the region.

Figure 3. Half-hourly rainfall data from one of the 51 monitoring locations, with capital letters (**A**) and (**B**) indicating the areas of influence from GPM-origin and WRF-origin, respectively. Points (**C**) and (**D**) denote the coordinates database for GPM-origin and WRF-origin, respectively. The discrepancies between datasets are evident when focusing on specific rainfall periods (outlined by the dotted square), namely July–August (a), early September (b), and winter season (c).

Observing Figure 3, it is notable that discrepancies exist between the GPM and WRF databases across various rainfall periods. These disparities may stem from multiple factors, including inherent uncertainties within both datasets. The complexity of forecasting convective and dominant precipitation events using the WRF model, could contribute to these observed differences [42]. Additionally, model-based products excel during cold seasons, while satellite-based products perform better during warm seasons [43]. Comparing WRF-modeled rainfall data with satellite-estimated data is a common practice in meteorological research and offers valuable insights into model performance. Sensitivity analyses and validation against ground-based observations typically enhance the robustness of such comparisons; unfortunately, ground-based observations are lacking in this study. These findings imply that the differences depicted in Figure 3 may be influenced by the season and type of precipitation. Further research is warranted to delve deeper into these factors.
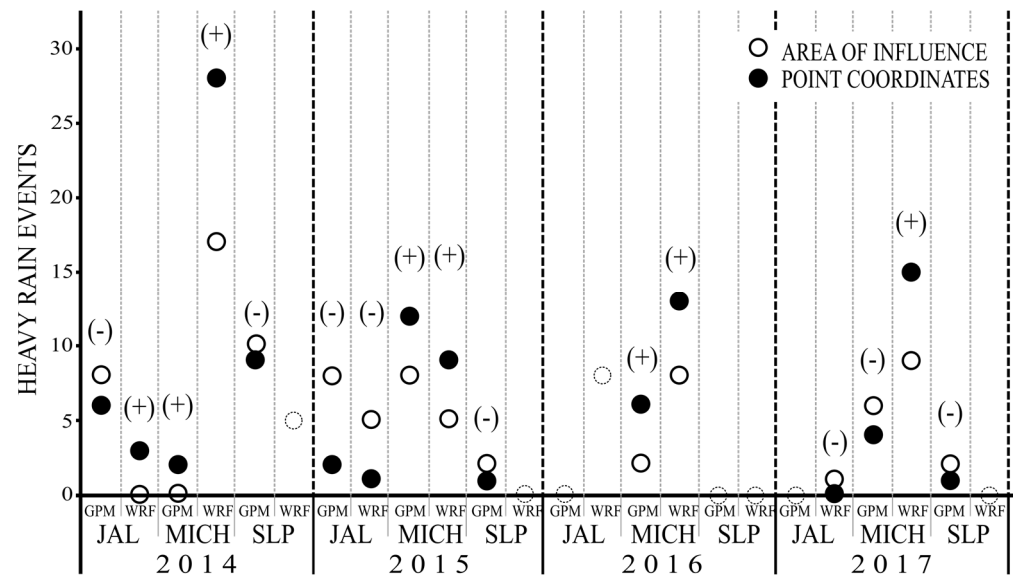
Figure 4. The annual ratio of heavy rain events by database, region, and year for both the area of influence and point coordinate data. The positive ratio (+) indicates that the number of heavy rain events was greater at the hail cannon location (pair coordinates) than in the area of influence, while the negative ratio (−) indicates the opposite, where the number of episodes within the 3 km of the area of influence was greater than in the hail cannon location. The dotted and filled circle symbols denote the same, representing the number of episodes by geographic feature.

3. Results

The data analysis showed that the MICH region had the highest number of heavy rain events in the period and experienced the highest number of events among regions. In 2014, 47 events were recorded in MICH (17 in JAL and 29 in SLP), followed by 34 events in 2015 (16 in JAL and 3 in SLP), 29 events in 2016 (16 in JAL and 0 in SLP), and 34 events in 2017 (1 in JAL and 3 in SLP). During the rainy season, which usually lasts from June to September, heavy rainfall was observed in all regions, with a clear dependence on the time of the year (July to August, early September, and winter season).

The differences between the databases and the geographic features were also significant. The algorithm identified a greater number of heavy rainfall events in the WRF database than in the GPM database. In the area of influence, 58 heavy rain events were observed in the WRF database, compared to 46 in the GPM database, while in the mask with point-to-point compensation analysis, 82 heavy rain events were observed in the WRF database, compared to 43 in the GPM database (unmatched *t* test = 0.0001; Figure 4). The MICH region had the largest number of heavy rain events in both databases, with 45 events observed in the WRF database and only 2 in the GPM database. The ratio of the number of heavy precipitation episodes was determined to illustrate the differences between databases, geographic regions, and geographic features (Figure 4).

The graph reveals that the number of heavy rain events varied greatly between the different regions and databases, as well as between geographic features. In general, the WRF database identified a greater number of heavy rain events compared to the GPM database. The MICH region had the highest number of events in the period, with the largest difference observed between databases.

The annual analysis shows that the maximum number of heavy rain events was recorded in 2014, with a decreasing trend in the following years. In addition, the differences between the geographic features were significant, with a higher number of events detected at the point coordinates than in the area of influence. This finding suggests that the hail cannon location is not the most suitable location for monitoring heavy rain events in the region.

Figure 4 shows that there is no visible trend or pattern between the two geographic features, despite the common belief in the protective role of hail cannons against the occurrence of hailstorms and heavy rain events. In addition, notable differences in the estimates of rainfall data between the databases are apparent (Figure 5).
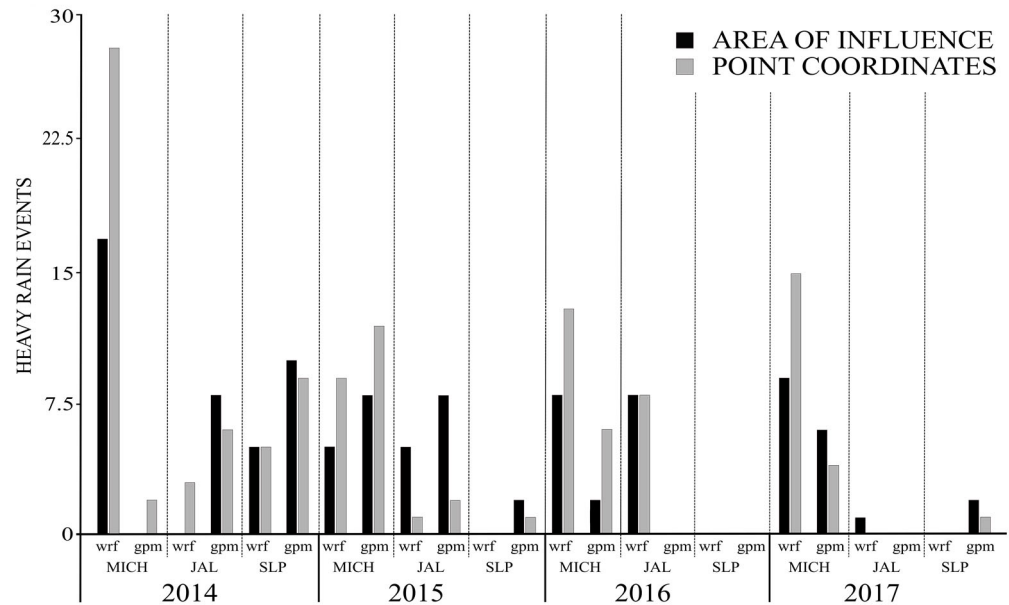
Figure 5. Summary of the number of heavy rain events detected on the location of the hail cannon and its area of influence. Representation on the x-axis is organized vertically in ascending order by year, region, and database origin.

It is important to note that the data presented in Figure 5 only show a correlation between the number of heavy rain events and the location of the hail cannon. Correlation does not imply causation, and further research would be necessary to determine if the hail cannon is actually impacting the rainfall in the region. It is also possible that other factors, such as local topography, may be influencing the distribution of heavy rain events in the area. Therefore, it is important to interpret these findings with caution and not draw definitive conclusions without further investigation.

4. Discussion

The extensive processing of large-scale data, including machine learning and data mining tasks, demands substantial computing resources [44], often facilitated by high-performance computing platforms and distributed frameworks such as Apache Hadoop and Spark. These resources enable parallel processing, accelerating data analysis. However, ensuring adequate computing power and storage capacity is essential. Scientifically, challenges arise in data quality, statistical inference, and reproducibility, being addressed through techniques such as data cleaning, statistical modeling, and version control systems. The lack of scientific evidence supporting the effectiveness of hail cannons in altering extreme rainfall events underscores the importance of relying on empirical data and scientific research. The controversy surrounding hail cannon usage and its uncertain environmental and weather impacts necessitates further research for a comprehensive understanding.

Our study focused on evaluating the relationship between heavy rain events and hail cannon locations, finding no evidence supporting hail cannons' dissipation or attenuation effects on heavy rain occurrence. Future research adjustments include matching data registration frequency with extreme rain event durations and incorporating additional weather device records near hail cannon locations, such as dual-polarization radar data. The dual-polarization radar can discern between heavy rains and hail conditions in the atmosphere. In orographic complex terrain, long-range radar estimations are not able to

identify the rain areas correctly due the blockage caused by mountains and the growth of low-level precipitation [45,46].

While hail events and heavy rainfall share similar atmospheric triggers, it is crucial to conduct rigorous scientific studies to establish any causal relationship between hail cannon activity and heavy rain occurrence. Further research should prioritize incorporating ground-based weather station networks to enhance dataset robustness.

The integration of multiple data sources and the use of code pipelines for automation contribute to a more comprehensive analysis, highlighting the importance of computing resources in large-scale data processing. This study emphasizes the need for efficient and scalable processing methods, as datasets grow in size and complexity [47].

However, the results of this study do not yield robust information to accurately determine any association between hail cannons operations and the occurrence of heavy rain events in the study regions. While manufacturers claim that hail cannons can dissipate hail formation and affect the process of storm cloud formation, there is no scientific evidence to support their claims. We reiterate that the lack of scientific literature on this topic is evident, and further research is needed. It is reasonable to associate different weather phenomena such as hail and convective storm because both events can be triggered by the same atmospheric conditions, particularly in the context of severe thunderstorms.

It is important to approach scientific studies with a critical and unbiased perspective and to base conclusions on rigorous experimental and observational evidence. While it is understandable that farmers may hold beliefs about the effectiveness of hail cannons in preventing hail formation and reducing rainfall intensity, it is important to evaluate these claims using scientific methods to determine their validity.

We proposed, for future studies, reasonable and necessary items to improve the understanding of the relationship between hail cannons and heavy rainfall events. Matching the frequency of data registration with the duration of extreme rain events (5 to 10 min [48]), would allow for a better exploration of the potential association between hail cannons and heavy rainfall events. Additionally, incorporating ground data from other weather devices [47] near the hail cannon location, such as rainfall, relative humidity, wind intensity, wind direction, and air temperature, would enrich the dataset and provide more comprehensive information for analysis.

However, the lack of willingness on the part of the owners of the hail cannon devices to share information about their operation frequency and period is a limitation that needs to be addressed. Obtaining this information would be important to better understand the potential effects of hail cannons on weather patterns.

In this study, the use of multiple data sources and an integrated data framework can improve the accuracy and reliability of large-scale data analysis. The relevance of multisource data integration might provide robust information on the scale at which hail cannons operate, compared to the scale of atmospheric processes that lead to heavy rainfall events. Hail cannons typically operate on a very localized scale, aiming to disrupt the formation of hailstones in a small area. In contrast, heavy rainfall events are often driven by large-scale atmospheric patterns and processes that are influenced by factors such as temperature gradients, moisture content, and air mass movements on regional or even global scales. The operation principle is that hail cannons operate by creating shockwaves or sound pulses that are intended to disrupt the formation of hailstones within thunderstorm clouds. While their primary aim is to reduce the size of hailstones, the energy produced by hail cannons could potentially interfere with atmospheric stability and cloud development. This disruption may alter the microphysical processes within clouds, potentially affecting precipitation patterns. In addition, while hail cannons may have some impact on local weather patterns, their effects are likely to be minimal compared to the complex interplay of atmospheric variables that contribute to heavy rainfall, such as moisture availability, instability, and lifting mechanisms. The use of hail cannons generates localized disturbances in the atmosphere, which could impact the vertical motion of air masses and cloud dynamics. These disturbances might influence the distribution

and intensity of precipitation in the immediate vicinity of the hail cannon deployment area. However, the extent of this influence would likely be limited to a relatively small spatial scale.

Acknowledging the limitations or uncertainties associated with our study, we note that these could include factors such as the availability of data, the accuracy of hail cannon usage records, or the complexity of atmospheric processes that were not fully accounted for in our analysis. In this study we have conducted research on the influence of hail cannons on precipitation. It is essential to provide a detailed statistical analysis of our findings. This could involve comparing precipitation data from periods when hail cannons were active versus inactive, while controlling for other relevant factors that may influence precipitation patterns.

5. Conclusions

Using the term "hail cannon" to specifically indicate its purpose in reducing the diameter of hail is appropriate, as these devices are primarily deployed to mitigate hail damage to crops, buildings, and other infrastructure. However, it is also important to consider how the operation of hail cannons might indirectly affect the amount of precipitation in a given area. While the primary purpose of hail cannons is to reduce hailstone size, their operation may indirectly affect precipitation patterns through localized atmospheric disturbances. However, the overall impact of hail cannons on precipitation amounts is likely to be minimal, compared to the broader atmospheric processes that govern weather and climate patterns. In the pursuit of understanding the effectiveness of hail cannon devices in influencing heavy rainfall events, this study has explored the intricate interplay between computing technology, spatial analysis, meteorological phenomena, and farmers' perceptions. Utilizing advanced spatial analysis techniques and leveraging two precipitation databases, our research sheds light on certain aspects of this multifaceted issue. While hail cannons may have some localized effects on precipitation patterns, their impact on the overall amount of precipitation in a region is likely to be minimal. Precipitation events are driven by a complex interplay of atmospheric factors such as moisture availability, temperature gradients, and atmospheric dynamics on regional or larger scales. The operation of hail cannons is unlikely to significantly alter these large-scale atmospheric processes.

Our findings indicate that the spatial distribution of heavy rainfall events at the hail cannons' location and within their area of influence were not related at all. However, it is crucial to acknowledge the limitations and complexities that persist in fully elucidating the role of hail cannons in weather modification.

Despite advancements in meteorological research, the effectiveness of hail cannons in altering precipitation patterns remains a contentious and scientifically intricate subject. Farmers' perceptions of these devices, often influenced by regional climate challenges and economic considerations, may not align with the nuanced realities revealed by our analysis.

It is paramount to recognize the need for continued research, encompassing a broader spectrum of variables, and possibly engaging with stakeholders, to comprehensively grasp the implications of hail cannon use. Bridging the gap between scientific understanding and farmers' perspectives requires a holistic approach that considers meteorological, socio-economic, and environmental factors.

In conclusion, our findings suggest that hail cannons' impact on precipitation remains uncertain, necessitating further research. By acknowledging this study's limitations and uncertainties, we underscore the importance of evidence-based decision-making in evaluating hail cannon efficacy and environmental impacts.

References

1. Changnon, S.A.; Ivens, J.L. History repeated: The forgotten hail cannons of Europe. *Bull. Am. Meteorol. Soc.* **1981**, *62*, 368–375. [CrossRef]
2. Plumandon, J.R. The third International Congress on hail shooting. In *Monthly Weather Review*; Encyclopedic Scientific des Aide-Memoire: Paris, France, 1902; Volume 30, pp. 33–35.
3. Changnon, S.A. On the status of hail suppression. *Bull. Am. Meteorol. Soc.* **1977**, *58*, 20–28. [CrossRef]
4. Guhathakurta, P.; Sreejith, O.P.; Menon, P.A. Impact of climate change on extreme rainfall events & flood risk in India. *J. Earth Syst.* **2011**, *120*, 359–373. [CrossRef]
5. Pall, P.; Aina, T.; Stone, D.; Stott, P.; Nozawa, T.; Hilberts, A.G.J.; Lohmann, D.; Allen, M.R. Anthropogenic greenhouse gas contribution to flood risk in England and Wales in autumn 2000. *Nature* **2011**, *470*, 382–385. [CrossRef]
6. Rajeevan, M.; Bhate, J.; Jaswal, A.K. Analysis of variability and trends of extreme rainfall events over India using 104 years of gridded daily rainfall data. *Geophys. Res. Lett.* **2008**, *35*, L18707.
7. Saura, J.R.; Ribeiro-Navarrete, S.; Palacios-Marqués, D.; Mardanni, A. Impact of extreme weather in production economics: Extracting evidence from user-generated content. *Int. J. Prod. Econ.* **2023**, *260*, 108861. [CrossRef]
8. Frame, D.J.; Rosier, S.M.; Noy, I.; Harrington, L.J.; Carey-Smith, T.; Sparrow, S.N.; Dean, S.M. Climate change attribution and the economic costs of extreme weather events: A study on damages from extreme rainfall and drought. *Clim. Chang.* **2020**, *162*, 781–797. [CrossRef]
9. Loriaux, J.M.; Lenderink, J.; Siebesma, A.P. Peak precipitation intensity in relation to atmospheric conditions & large-scale forcing at midlatitudes. *J. Geophys. Res. Atmos.* **2016**, *121*, 5471–5487. [CrossRef]
10. Ripple, W.J.; Wolf, C.; Gregg, J.W.; Levin, K.; Rockström, J.; Newsome, T.M.; Lenton, T.M. World scientists' warning of a climate emergency 2022. *Bioscience* **2022**, *72*, 1149–1155. [CrossRef]
11. Kong, A. Another Year for the Record Books: A Recap of the Main Extreme Weather Events in Summer 2023. Available online: https://earth.org/another-year-for-the-record-books-a-recap-of-the-main-extreme-weather-events-in-summer-2023/ (accessed on 27 May 2024).
12. Cică, R.; Burcea, S.; Bojariu, R. Assessment of severe hailstorms & hail risk using Weather radar data. *Meteorol. Appl.* **2015**, *22*, 746–753. [CrossRef]
13. Adams, D.K.; Comrie, A. The North American monsoon. *Bull. Am. Meteorol. Soc.* **1997**, *78*, 2197–2213. [CrossRef]
14. Higgins, R.W.; Shi, W. Dominant factors responsible for interannual variability of the summer monsoon in the southwestern United States. *J. Clim.* **2000**, *13*, 759–776. [CrossRef]
15. Aramyan, A.R.; Aramyan, G.R.; Haroyan, K.P.; Galechyan, G.A.; Vardanyan, A.A.; Danielyan, G.A.; Nersisyan, H.B.; Bilen, S. A study of acoustic waves generated by the shock wave of an anti-hail gun. *Acoust. Phys.* **2011**, *57*, 432–436. [CrossRef]
16. Sage, A. Anti-Hail Cannon Fail to Protect Vineyards. 2020. Available online: https://www.thetimes.co.uk/edition/news/anti-hail-cannon-fail-to-protect-vineyards-m06lwv0ss (accessed on 30 September 2020).
17. Birsan, M.; Muscalu, A.; Voicea, I.; Pruteanu, A. General aspects of the extreme meteorological phenomenon: Hail. *Ann. Fac. Eng. Hunedoara Int. J. Eng.* **2019**, *17*, 81–88.
18. INEGI Atlas de Huracanes en el Océano Pacífico y el Océano Atlántico. 1979. Available online: https://en.www.inegi.org.mx/contenidos/productos/prod_serv/contenidos/espanol/bvinegi/productos/historicos/2104/702825220150/702825220150_1.pdf (accessed on 22 May 2024).
19. Pandas Ecosystem. 2020. Available online: https://pandas.pydata.org/community/ecosystem.html (accessed on 1 October 2020).

20. Seneviratne, S.I.; Nicholls, N.; Easterling, D.; Goodess, C.M.; Kanae, S.; Kossin, J.; Luo, Y.; Marengo, J.; McInnes, K.; Rahimi, M.; et al. Changes in climate extremes & their impacts on the natural physical environment. In *Managing the Risks of Extreme Events & Disasters to Advance Climate Change Adaptation*; Field, C.B., Barros, V., Stocker, T.F., Qin, D., Dokken, D.J., Ebi, K.L., Mastrandrea, M.D., Mach, K.J., Plattner, G.-K., Allen, S.K., Eds.; A Special Report of Working Groups I & II of the Intergovernmental Panel on Climate Change (IPCC); Cambridge University Press: Cambridge, UK; New York, NY, USA, 2012; pp. 109–230.

21. Servicio Meteorológico Nacional. Glosario Técnico. Available online: https://smn.conagua.gob.mx/es/smn/glosario#:~:text=Lluvia%20fuerte,%20abundante,%20repentina%20y%20de%20poca%20duraci%C3%B3n (accessed on 22 May 2024).

22. Huffman, G.J.; Bolvin, D.T.; Nelkin, E.J. *Integrated Multi-SatellitE Retrievals for GPM (IMERG) Technical Documentation*; _3imerg Goddard Space Flight Center: Greenbelt, MD, USA, 2017. Available online: https://gpm.nasa.gov/sites/default/files/document_files/IMERG_doc.pdf (accessed on 21 July 2020).

23. Yi, L.; Zhang, W.; Wang, K. Evaluation of Heavy Precipitation Simulated by the WRF Model Using 4D-Var Data Assimilation with TRMM 3B42 & GPM IMERG over the Huaihe River Basin, China. *Remote Sens.* **2018**, *10*, 646. [CrossRef]

24. NASA. GPM Completes Five Years of Operation. 2019. Available online: https://www.un-spider.org/news-and-events/news/gpm-completes-five-years-operations (accessed on 27 May 2024).

25. Roy, A.; Thakur, P.K.; Pokhriyal, N.; Aggarwal, S.P. Intercomparison of different rainfall products and validation of wrf modelled rainfall estimation in n-w Himalaya during monsoon period. *ISPRS Ann. Photogramm. Remote Sens. Spat. Inf. Sci.* **2018**, *4*, 351–358. [CrossRef]

26. Skamarock, W.C.; Klemp, J.B.; Dudhia, J.; Gill, D.O.; Barker, D.M.; Duda, M.G.; Huang, X.Y.; Wang, W.; Powers, J.G. A Description of the Advanced Research WRF Version 3. (No. NCAR/TN-475+STR). University Corporation for Atmospheric Research: Boulder, CO, USA, 2008. [CrossRef]

27. Janjić, Z.I. The step-mountain Eta coordinate model: Further developments of the convection, viscous sublayer, & turbulence closure schemes. *Mon. Weather Rev.* **1994**, *122*, 927–945.

28. Thompson, G.; Rasmussen, R.M.; Manning, K. Explicit forecasts of winter precipitation using an improved bulk microphysics scheme, Part I: Description and sensitivity analysis. *Mon. Weather Rev.* **2004**, *132*, 519–542. [CrossRef]

29. Janjić, Z.I. Nonsingular implementation of the Mellor-Yamada level 2.5 scheme in the NCEP meso model. In *NCEP Office Note No. 437*; National Center of Environmentral Prediction: College Park, MD, USA, 2002; 61p.

30. Tewari, M.; Chen, F.; Wang, W.; Dudhia, J. Implementation and verification of the unified NOAH land surface model in the WRF model. In Proceedings of the 20th Conference on Weather Analysis and Forecasting/16th Conference on Numerical Weather Prediction, Seattle, WA, USA, 12–16 January 2004; pp. 11–15.

31. Vaidya, S.S.; Singh, S.S. Applying the Betts-Miller-Jancic scheme of convection on prediction of the Indian Monsoon. *Am. Meteorol. Soc.* **2000**, *15*, 349–356.

32. Sari, F.P.; Baskoro, A.P.; Hakim, O.S. Effect of different microphysics scheme on WRF model: A simulation of hail event study case in Surabaya, Indonesia. *AIP Conf. Proc.* **2018**, *1987*, 020002. [CrossRef]

33. Jia, W.; Zhang, X. The role of the planetary boundary layer parameterization schemes on the meteorological and aerosol pollution simulations: A review. *Atmos. Res.* **2020**, *239*, 1250. [CrossRef]

34. González-Rocha, S.N.; Juárez-Pérez, F.; Aguilar-Meléndez, A.; Cristóbal Salas, A.; Calderón-Ramón, C.; Escalante-Martínez, J.E.; Baldasano Recio, J.M. Planet Boundary Layer Parameterization in Weather Research & Forecasting (WRFv3.5): Assessment of Performance in High Spatial Resolution Simulations in Complex Topography of Mexico. *Comput. Sist.* **2017**, *21*, 35–44. [CrossRef]

35. Bowling, L.C.; Lettenmaier, D.P.; Nijssen, B.; Graham, L.P. Simulation of high-latitude hydrologic responses in the Torne-Kalix Basin: PILPS Phase 2(e): 1. Experiment description & summary intercomparisons. *Global Planet Change* **2003**, *38*, 1–30. [CrossRef]

36. Slater, A.G.; Bohn, T.J.; McCreight, J.L.; Serreze, M.C.; Lettenmaier, D.P. A multimodel Simulation of pan-Arctic hydrology. *J. Gephys. Res.* **2007**, *112*, G04S45. [CrossRef]

37. Arnaud, M.; Emery, X. *Estimation et Interpolation Spatiale*; Hermes Science Publication: Paris, France, 2000.

38. Klinkenberg, B.; Waters, N.M. Unit 40. Spatial Interpolation I. 2018. Available online: https://escholarship.org/uc/item/02p486cx (accessed on 29 May 2018).

39. Matthews, S.A. *ArcGIS Geostatistical Analyst, GIS Resource Document*; ESRI: Redlands, CA, USA, 2002. Available online: https://help.arcgis.com/en/arcgisdesktop/10.0/pdf/geostatistical-analyst-tutorial.pdf (accessed on 4 May 2023).

40. Python Language Reference. Scipy 1.4.1. Project Description. Released 19 December 2019. 2019. Available online: https://pypi.org/project/scipy/ (accessed on 31 January 2019).

41. Bates, P.D.; De Roo, A.P.J. A simple raster-based model for flood inundation simulation. *J. Hydrol.* **2000**, *236*, 54–77. [CrossRef]

42. Lin, L.F.; Ebtehaj, A.M.; Bras, R.L.; Flores, A.N.; Wang, J.F. Dynamical precipitation downscaling for hydrologic applications using WRF 4D-Var data assimilation: Implications for GPM era. *J. Hydrometeorol.* **2015**, *16*, 811–829. [CrossRef]

43. Zhang, J.; Lin, L.-F.; Bras, R.L. Evaluation of the Quality of Precipitation Products: A Case Study Using WRF & IMERG Data over the Central United States. *J. Hydrometeorol.* **2018**, *19*, 2007–2020. [CrossRef]

44. Fungtammasan, A.; Lee, A.; Taroni, J.; Wheeler, K.; Chin, C.S.; Davis, S.; Greene, C. Ten simple rules for large-scale data processing. *Comput. Biol.* **2022**, *18*, e1009757. [CrossRef]

45. Michaelides, S. Remote Sensing of Precipitation. *Remote Sens.* **2019**, *11*, 389. [CrossRef]

46. Zhang, J.; Qi, Y.; Kingsmill, D.; Howard, K. Radar-based quantitative precipitation estimation for the cool season in complex terrain: Case studies from the NOAA hydrometeorology test bed. *J. Hydrometeorol.* **2012**, *13*, 1836–1854. [CrossRef]

47. Snijders, C.; Matzat, U.; Reips, U.D. "Big Data": Big Gaps of Knowledge in the Field of Internet Science. *Int. J. Internet Sci.* **2012**, *7*, 1–5.

48. Garcia-Bartual, R.; Schneider, M. Estimating maximum expected short-duration rainfall intensities from extreme convective storms. *Phys. Chem. Earth Part B Hydrol. Ocean. Atmos.* **2001**, *26*, 675–681. [CrossRef]